

# AN ITERATIVE METHOD FOR REGISTRATION OF HIGH-RESOLUTION CARDIAC HISTOANATOMICAL AND MRI IMAGES

*Tahir Mansoori<sup>1</sup>, Gernot Plank<sup>2</sup>, Rebecca Burton<sup>3</sup>, Jürgen Schneider<sup>4</sup>,  
Peter Kohl<sup>3</sup>, David Gavaghan<sup>5</sup>, Vicente Grau<sup>6</sup>*

<sup>1</sup>Life Sciences Interface Doctoral Training Centre, University of Oxford, OX1 3QD, UK

<sup>2</sup>Institute of Biophysics, Medical University of Graz, 8010 Graz, Austria

<sup>3</sup>Department of Physiology Anatomy and Genetics, University of Oxford, OX1 3PT, UK

<sup>4</sup>Department of Cardiovascular Medicine, University of Oxford, Oxford, OX3 7BN, UK

<sup>5</sup>Oxford University Computing Laboratory, OX1 3QD, UK

<sup>6</sup>Department of Engineering Science, University of Oxford, OX1 3PJ, UK

## ABSTRACT

Cardiac computational models of electrical conduction, mechanical activation, hemodynamics and metabolism require detailed information about the structural arrangement of functionally heterogeneous cardiac cell types. However, current state-of-the-art models lack anatomically accurate cell type localization, which limits their utility. Histological sections combine unique resolution with discrimination of tissues and anatomical structures, but they suffer from alignment and deformation problems. On the other hand, MRI datasets preserve the correct geometry, but provide less micro structural detail. This paper presents a method for aligning MRI and histological datasets to obtain a highly detailed, geometrically correct anatomical description of the heart. An iterative process is used to correct the various 2D and 3D, rigid and non-rigid transforms, introduced in the histology preparation and acquisition. Validation is performed by calculating distances between anatomical landmarks in both datasets, and by quantifying tissue overlap. Results illustrate the suitability of the proposed algorithm to produce detailed, accurate cardiac models.

## 1. INTRODUCTION

Anatomical and functional information about cardiac structures is fundamental to understand mechanisms at play in both healthy and pathological hearts. However, even after more than a century of studies into ventricular tissue architecture, there is still controversy about apparently basic issues, such as whether or not there is a ‘unique band’ arrangement of myocardial fibres throughout the heart. Furthermore, electromechanical models of the heart can provide unique insight into the intricate complexity of cell

type distribution, mechano-electrical activation, hemodynamics, and metabolism in the normal and diseased heart. Cardiac computational models require detailed information about cardiac anatomy, cell type heterogeneity and distribution, the Purkinje fiber system, coronary vasculature, fiber orientation, cardiac sheet structure, and material properties of cardiac tissues. However, to date the work carried out in cardiac modelling has used overly simplified descriptions of the heart, hindering efforts to obtain realistic simulation results.

The absence of highly detailed models of cardiac anatomy may be due to the difficulty in obtaining three-dimensional images of the whole heart at sufficiently high resolution. Non-invasive medical imaging techniques, such as MRI and CT, provide anatomically correct images, but they have limited resolution and do not allow discrimination of all cell types. On the other hand, histological datasets provide sufficient resolution and tissue discrimination power, but they are ‘destructive’ and, due to the fixing and slicing process, they contain significant slice-to-slice misalignments and non-rigid deformations that make building a correct three-dimensional model difficult. Combining histological data with MRI potentially brings the best of both worlds, making it possible to obtain highly detailed anatomical images, while minimizing geometrical distortion. In this paper, we propose a registration algorithm that enables one to align histological slices to 3D MRI data, correcting the various rigid and non-rigid deformation sources.

Preliminary work by our group [1] discussed the development of computational models of individual hearts using histology and MRI at unprecedented resolution. An optical flow method was employed to perform inter-slice registration of histology images. While this approach, which is generally applied for correction of distortion in histological images [2], is capable of correcting major

misalignments, it has an important drawback: by aligning adjacent slices we are reducing inter-slice differences that might be fundamental in the description of heart anatomy.

The work presented here uses an iterative procedure, which utilizes geometrically correct information available from MRI to perform histo-anatomical registration to establish 3D correspondence between MRI and histology.

Previous publications most closely related to our work include [3,4,5]. However, only affine and rigid transformations are used in [3,4], while an extra dataset is used to find orientation of histology in [5]. These references describe work on brain images; to our knowledge, this is the first time this technique has been applied in the cardiac field. Anatomical models of ventricular anatomy with fiber orientations have been generated at lower resolution using only MRI/DTMRI [6,7] but these models lack micro-structural detail and cell type discrimination. The details of the method are given in Section 2.2. Once the 3D correspondence is established, cell types are identified in histology using CIELAB color space thresholding, and mapped to MRI to form anatomically accurate meshes, enriched with heterogeneous cell type information.

## 2. METHODS

### 2.1 Data Acquisition

The data acquisition was led by the Cardiac Mechano-Electrical Feedback Group, Department of Physiology, Anatomy & Genetics, Oxford. Figure 1 is a schematic representation of the steps from heart isolation to the acquisition of MRI and histological images, including sources of deformation ( $T_i$ ). Hearts were isolated from female New Zealand white rabbits after cervical dislocation (UK Home Office guidance on the Operation of the Animals Scientific Procedures act of 1986) and cannulated via the aorta to a Langendorff perfusion system. Heart fixation was performed during cardioplegic arrest, and the fixed heart was stabilized in a 30mm NMR tube using low melting 1% agar and Gadodiamide contrast agent.

MRI scans were acquired with an 11.7 T, 500 MHz scanner at  $26.5 \times 26.5 \times 24.5 \mu\text{m}$  resolution, before histological sectioning. Increasing concentrations of alcohol were used to dehydrate the heart before embedding in wax [1]. Up to this point, intervening deformation sources  $T_1$  to  $T_3$  are all three-dimensional and non-rigid. The whole heart was serially sectioned at  $10 \mu\text{m}$  thickness using a microtome. Histology sectioning introduces further interslice 2D misalignments, and individual nonrigid deformations for each slice are represented by  $T_4$  in Figure 1. Every 5<sup>th</sup> section was Trichrome stained after relaxation and re-hydration (non-rigid, slice-specific 2D deformations,  $T_5$  and  $T_6$ ). Histology imaging was performed using a 5x objective with  $1.1 \mu\text{m}$  resolution. Full details of the experimental setup can be found in [1].

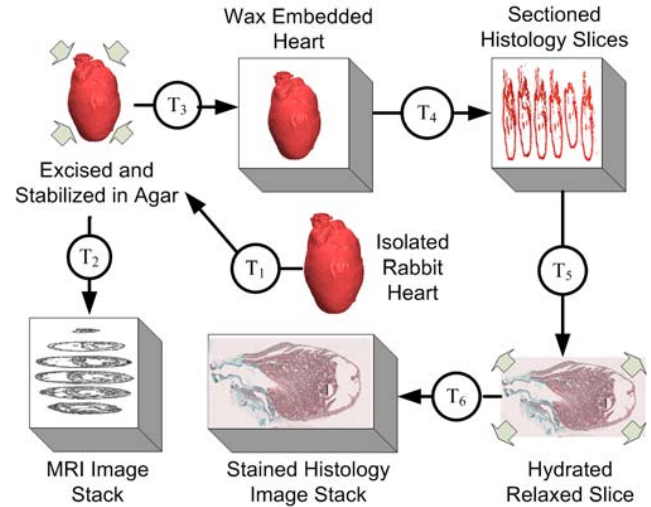


**Figure 1.** Cardiac imaging process and transformations showing deformations at each step

### 2.2 Iterative Histo-Anatomical Registration

Several geometrical transforms appear in the process of isolating, fixing, slicing and imaging the heart, as shown in Figure 1. These include a combination of 2D and 3D, rigid and non-rigid transforms. In order to reduce the complexity of the optimization procedure, we identified the components of the transform and solved them in an iterative procedure. The details of the method are outlined in Figure 2.

Histology slices were stacked together to form a volume, which was used to find the transformation  $J_1$  to get an initial alignment with the MRI volume.  $J_1$  is a 3D rigid transformation, which was calculated using a gradient descent optimizer and the mutual information similarity metric. An additional initial interslice alignment, as in [1], might be useful if the slices are strongly misaligned. In our case, slices were approximately aligned in the imaging process, and this preliminary step was not necessary. Once an approximate 3D correspondence between histology and MRI was found,  $J_2$  was applied to perform 2D rigid registration of each histology slice to the MRI slice extracted at the corresponding spatial location.  $J_2$  is a 2D rigid transformation, which was calculated using a gradient descent optimizer by maximizing mutual information between MRI and histology slices. This step solves the problem of misalignment between slices but, different to pure interslice alignment as used in [1], it preserves the differences between slices by using the 3D geometry from the MRI dataset. This procedure is repeated until the algorithm finds the optimal rigid registration between the two volumes using mutual information similarity metric. At this stage, corresponding MRI and histology slices can be extracted and non rigid histology to MRI slice registration is performed to calculate  $J_3$ . We solve the non-rigid registration problem using the Demons algorithm [8]. This

technique, as with other optic flow methods, assumes equal intensities between the two images. Histogram matching, applied as a preliminary step, proved to be sufficient to fulfill this requirement.

It is important to note that the non rigid transform  $J_3$  is placed outside of the iterative loop. This is due to the fact that this transform would be able to register any pair of MRI-histology slices, even if they do not correspond to the same anatomical locations, thus effectively leading to an incorrect solution. To avoid this error, we first calculate the optimal combination of rigid transforms and we allow non-rigid deformation only as a last step.

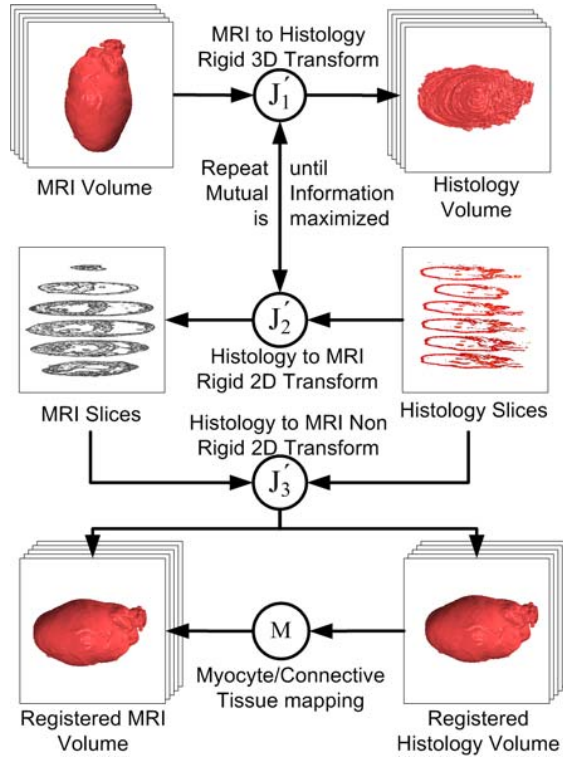


**Figure 2.** Representation of the iterative registration method, showing the different transforms.

### 2.3 Cell Type Mapping

One of the main goals of our work was to accurately identify the location of different cell types. Histology slices are stained to discriminate myocytes and connective tissue which are discernible as red / green structures respectively, as shown in Figure 5a. To exploit this property, we transformed the histology images from the RGB to the CIELAB color space, which is based on human eye perception. Of the three  $L^*a^*b^*$ , defined by the CIELAB space, the  $a^*$  component, which divides the color axis between magenta and green, was used for discrimination. A double threshold was used on the  $a^*$  channel to discriminate between connective tissue, background and myocytes.

### 3. RESULTS AND DISCUSSION

The iterative process described in Section 2.2 was applied to histological and MRI datasets, acquired as explained in Section 2.1. The histological dataset was downsampled to  $512 \times 512 \times 400$  voxels with  $53 \times 53 \times 49 \mu\text{m}$  resolution, to assure computational tractability. The iterative process was run until convergence, which in our experiments occurred after 4 iterations.

In Figure 3(a), the average values for rotation angle and translation for the 2D rigid transforms are shown. Figure 3(b) shows the mutual information values for the 3D transform  $J_1$ . Note that between two calculations of  $J_1$ , jumps in the mutual information value appear: this corresponds to the application of the 2D transforms  $J_2$ . Figure 4 shows the result of the registration procedure.

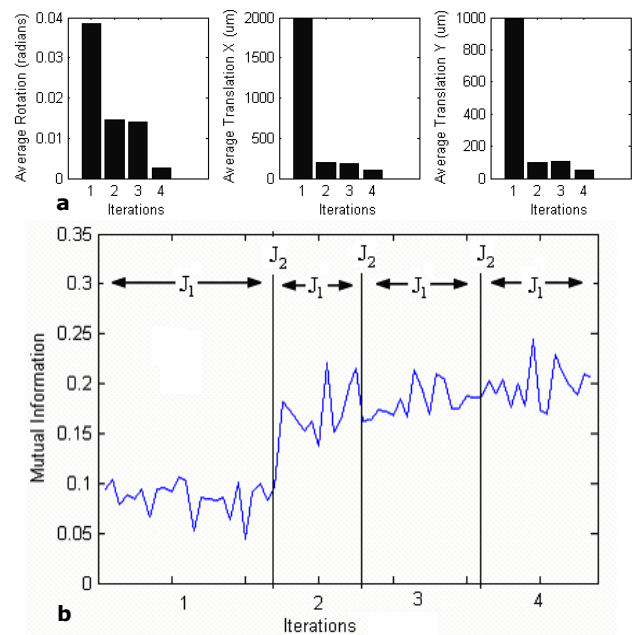


**Figure 3.** Illustration of the behavior of the iterative registration process. (a) Average translation and rotation values of the 2D transform. (b) Evolution of the mutual information value.

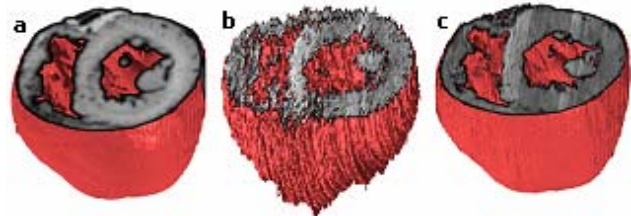


**Figure 4.** Results of 3D correspondence after histo-anatomical registration. a) 3D MRI volumes showing cross section through ventricles b) Associated histology volume with deformations c) Histology volume after registration

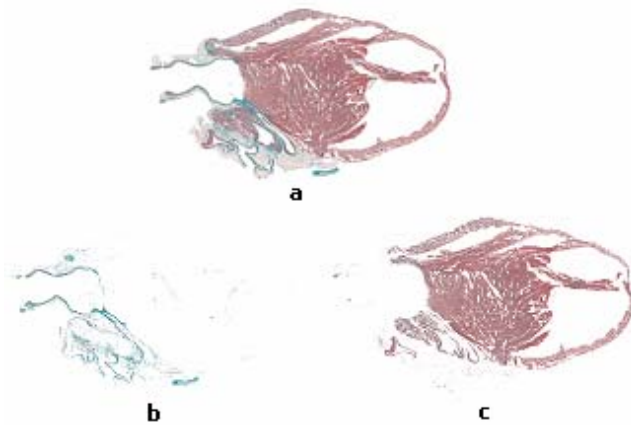


**Figure 5.** Results of connective tissue/myocyte segmentation. a) Stained histology slice; b, c) a\* thresholding of connective tissue and myocytes.

Figure 5 shows the results of segmentation of connective tissue and myocytes, in the corrected images. Two accuracy measures were calculated to validate the procedure. First, a physiologist selected corresponding landmarks in the original MRI and histology slices, and the distance between the landmarks after registration was calculated. In a first session, 50 landmarks, visible in both modalities, were identified. In a second session, landmarks were identified again in the histological images, in order to obtain a measure of variability. The mean Euclidian distance between corresponding landmarks was found to be 0.24 mm, i.e. 4.4 pixels. The expert variability between two sessions was found to be 0.04 mm. The distance between landmarks in the registered datasets might be due to the presence of areas of approximately constant intensity, where it is difficult to find exact point-to-point correspondences. A second validation measure, not depending on manual landmark location, was obtained by calculating the tissue overlap in the aligned images. The datasets were thresholded, and the Dice coefficient was calculated. The Dice coefficient provides a figure between 0 and 1, with 1 corresponding to perfect overlap. A value of 0.988 was obtained for the aligned datasets.

Wax embedding might introduce 3D deformation of the specimen, which would produce out of plane tilting and warping in the histological slices. The presented algorithm does not correct for these deformations, as we believe they will have a negligible effect in the final result. This is confirmed by visual inspection and the quantitative results presented above. In histology datasets with significant out of plane tilting and warping, an additional 3D non rigid registration step can be introduced to reduce correspondence error between MRI and histology.

The anatomically correct histological models, obtained using the algorithm described here, constitute a unique resource to understand the microscopic make-up of

the heart, and to quantify its variability. Furthermore, they can be used to build highly detailed electromechanical cardiac models. Our current work includes applying the presented algorithm to a collection of histological-MRI pairs from different subjects, to obtain a statistical description of the cardiac anatomy, and developing inter-subject registration algorithms.

**Acknowledgements:** The authors would like to thank Professor Sir Michael Brady, Wolfson Medical Vision Lab, University of Oxford for his valuable comments. This research was supported by BBSRC.

#### 4. REFERENCES

- [1] R. Burton, G. Plank, J. Schneider, J. Prassl, J. Lee, V. Grau, N. Smith, N. Trayanova, P. P. Kohl, H. Ahammer and S. Keeling. "3-Dimensional Models of Individual Cardiac Histo-Anatomy: Tools and Challenges". *Annals of the New York Academy of Sciences*, 2006.
- [2] S.L. Keeling and W. Ring. "Medical Image Registration and Interpolation by Optical Flow with Maximal Rigidity". *Journal of Mathematical Imaging and Vision*, vol 23, no 1, pp. 47-65, 2005.
- [3] G. Malandain, E. Bardinet and K. Nelissen, W. Vanduffel. "Fusion of autoradiographs with an MR volume using 2-D and 3-D linear transformations", *Neuroimage*, pp. 111-27, 2004.
- [4] S. Ourselin, E. Bardinet, D. Dormont, G. Malandain, A. Roche, N. Ayache, D. Tandé, K. Parain and J. Yelnik. "Fusion of Histological Sections and MR Images: Towards the Construction of an Atlas of the Human Basal Ganglia", *In Proceedings of Medical Image Computing and Computer-Assisted Intervention*, 2001.
- [5] T. Schormann and K Zilles. "Three-dimensional Linear and Nonlinear Transformations: An Integration of Light Microscopical and MRI Data", *Human Brain Mapping*, pp. 339, 1998.
- [6] P. Helm, M. Beg, M. Miller and R. Winslow. "Measuring and Mapping Cardiac Fiber and Laminar Architecture Using Diffusion Tensor MR Imaging". *Annals of the New York Academy of Sciences*, vol 1047, pp. 296-307, 2005.
- [7] D. Scollan, A. Holmes, J. Zhang and R. Winslow. "Reconstruction of cardiac ventricular geometry and fiber orientation using magnetic resonance imaging". *Annals of Biomedical Engineering.*, vol 28, no 8, pp. 934-944, 2000.
- [8] J.P. Thirion. "Fast Non-Rigid Matching of 3D Medical Images", *In Proceedings of the Conference on Medical Robotics and Computer Assisted Surgery*, 1995.